Design of a Current Controller Based on a Two Step Procedure for Grid-Connected Converters

Everson Mattos[1], Lucas C. Borin[1], Caio R. D. Osório[1], Gustavo G. Koch[2], Vinícius F. Montagner[1]
[1]Federal University of Santa Maria - UFSM - Santa Maria - RS - Brazil
[2]Federal University of Rio Grande do Sul - UFRGS - Porto Alegre - RS - Brazil
Email: everson.mattos@gmail.com

***Abstract*—This paper provides a two step procedure for current control design of grid-connected converters with LCL filter. The proposed procedure is based on: i) an internal loop with state feedback, aiming on active damping of the LCL filter resonance; ii) an external loop with resonant controllers, aiming to ensure tracking of sinusoidal grid current references. The state feedback gains are computed based on pole location and the resonant control gains are computed based on the minimization of a closed-loop tracking error index. A case study is shown to illustrate that the proposed control design procedure leads to grid-injected currents with suitable steady state and transient performances.**

***Keywords* – Active damping, Grid-connected converter, LCL filter, Resonant controller, State feedback control.**

I. Introduction

Renewable energy sources can help to supply the demand for electrical energy. In the connection of alternative sources to the grid, one has that issues such as synchronization and regulation of voltage, frequency and current become very important, with codes and standards that provide limits for the electrical variables. In this sense, the control of grid-connected converters (GCCs) has driven attention in industry and academy [1]–[4].

One important class of GCCs include voltage source inverters connected to the grid by means of LCL filters. These filters are known to provide good rejection of harmonics, but also exhibit a resonance peak that must be damped in order to avoid instability [5]–[13]. In this context, state feedback control can be used to increase the damping of the closed-loop system, as well to ensure tracking of references and rejection of disturbances [14]. This technique can be related to robust and optimal control [15], and was used in the current control of GCCs, for instance, in [16]–[20]. These works use robust pole location to assign the discrete-time closed-loop poles inside the unit circle for an entire set of uncertainties in the grid impedance. However, since the poles associated with the LCL filter and the poles associated with the resonant controllers are constrained together, the use of different criteria to damp the resonance of the filter and to design the gains of resonant controllers is an interesting feature, that have not been explored in these works.

This paper proposes a two step procedure for current control design of GCCs with LCL filter, based on state feedback of the filter states and on resonant controllers. The proposed procedure is based on a state space model of the converter, including one sample delay in the discretization of the plant, and also in the state space representation of resonant controllers. The internal loop is comprised by a state feedback controller that ensures damping of the resonance of the LCL filter, including the effect of the delay. The external loop includes a resonant controller to ensure tracking error minimization given sinusoidal references for the grid current and also the rejection of grid voltage disturbances.

II. Plant model

Consider a GCC comprised by a voltage source inverter, an LCL filter and a predominantly inductive grid, as given in Fig. 1. It is assumed that the input DC voltage and the synchronization with the voltage at the point of common coupling (PCC) are ensured by suitable strategies [4], [21], [22]. Therefore, the objective here is to regulate the grid injected currents, i_g.

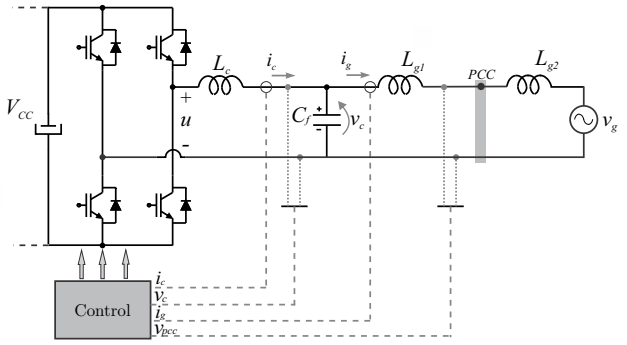

Figure 1. Inverter connected to the grid through an LCL filter.

Taking into account that the signal u is the control signal to be synthesized, and that the inductances at the PCC can be summed up for sake of modeling, the GCC in Fig. 1 can be represented in a simplified way as it is shown in Figure 2.

From Fig. 2, one state space model can be written, using the inductor currents and capacitor voltage as state variables, and the grid voltage as a disturbance, as given by

$$\begin{aligned} \dot{\mathbf{x}} &= \mathbf{A}\mathbf{x} + \mathbf{B}_u u + \mathbf{B}_g v_g \\ y &= \mathbf{C}\,\mathbf{x} \end{aligned} \tag{1}$$

https://doi.org/10.53316/sepoc2021.053

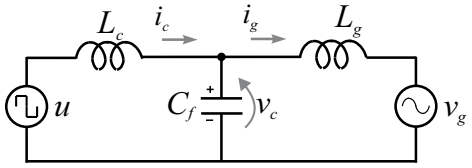

Figure 2. Simplified circuit used for plant modeling.

where

$$\mathbf{A}=\begin{bmatrix} 0 & -\frac{1}{L_c} & 0 \\ \frac{1}{C_f} & 0 & -\frac{1}{C_f} \\ 0 & \frac{1}{L_g} & 0 \end{bmatrix},\ \mathbf{B}_u=\begin{bmatrix} \frac{1}{L_c} \\ 0 \\ 0 \end{bmatrix},$$
$$\mathbf{B}_g=\begin{bmatrix} 0 \\ 0 \\ -\frac{1}{L_g} \end{bmatrix},\ \mathbf{x}=\begin{bmatrix} i_c \\ v_c \\ i_g \end{bmatrix},\ \mathbf{C}=\begin{bmatrix} 0 & 0 & 1 \end{bmatrix} \tag{2}$$

and $L_g = L_{g1} + L_{g2}$.

Aiming on the application of a digital control law, the plant model in (1)-(2) can be discretized, using the ZOH method, including one sample delay from the digital implementation of the control law, as [23]

$$\begin{aligned} \mathbf{x}(k+1) &= \mathbf{A}_d\mathbf{x}(k) + \mathbf{B}_{ud}\phi(k) + \mathbf{B}_{gd}v_g(k) \\ \phi(k+1) &= u(k) \end{aligned} \tag{3}$$

with

$$\mathbf{A}_d = e^{\mathbf{A}T_s},\ \mathbf{B}_{ud} = \int_0^{T_s} e^{\mathbf{A}\tau}\mathbf{B}_u d\tau,\ \mathbf{B}_{gd} = \int_0^{T_s} e^{\mathbf{A}\tau}\mathbf{B}_g d\tau \tag{4}$$

From (3) and (4) one can write

$$\begin{aligned} \mathbf{x}_d(k+1) &= \mathbf{G}_d\mathbf{x}_d(k) + \mathbf{H}_{ud}u(k) + \mathbf{H}_{gd}v_g(k) \\ \mathbf{y}(k) &= \mathbf{C}_d\mathbf{x}_d(k) \end{aligned} \tag{5}$$

where

$$\mathbf{G}_d=\begin{bmatrix} \mathbf{A}_d & \mathbf{B}_{ud} \\ \mathbf{0} & 0 \end{bmatrix},\ \mathbf{H}_{ud}=\begin{bmatrix} \mathbf{0} \\ 1 \end{bmatrix},\ \mathbf{H}_{gd}=\begin{bmatrix} \mathbf{B}_{gd} \\ 0 \end{bmatrix},$$
$$\mathbf{C}_d=\begin{bmatrix} \mathbf{C} & 0 \end{bmatrix},\ \mathbf{x}_d(k)=\begin{bmatrix} i_c(k) & v_c(k) & i_g(k) & \phi(k) \end{bmatrix}^T \tag{6}$$

III. Design of the controller in two steps

Consider the control system given in Fig. 3. This control system is comprised by two control loops. One internal loop, based on state feedback, and one external loop, based on a resonant controller.

The block representing the plant discretized including one sample delay has as inputs the disturbance (grid voltage v_g) and the control signal u. This control signal is composed by two terms: one state feedback action, u_{sf}, and one resonant action u_r.

For the control action u_{sf}, it is assumed that all filter state variables are available for feedback. For the control action u_r, it is assumed that the tracking error, with respect to a reference for the grid current i_g, is available.

The resonant controller can be represented in state space in discrete-time as [18], [20]

$$\begin{aligned} \boldsymbol{\rho}(k+1) &= \mathbf{R}_d\boldsymbol{\rho}(k) + \mathbf{S}_d e(k) \\ u_r(k) &= \mathbf{T}_d\boldsymbol{\rho}(k) \end{aligned} \tag{7}$$

where

$$\mathbf{R}_d = e^{\mathbf{R}T_s},\ \mathbf{S}_d = \int_0^{T_s} e^{\mathbf{R}\tau}\mathbf{S}_u d\tau,\ \mathbf{T}_d = \begin{bmatrix} K_{r1} & K_{r2} \end{bmatrix} \tag{8}$$

and

$$\mathbf{R}=\begin{bmatrix} 0 & 1 \\ -\omega_n^2 & -2\xi\omega_n \end{bmatrix},\ \mathbf{S}=\begin{bmatrix} 0 \\ 1 \end{bmatrix} \tag{9}$$

The proposed procedure for the design of the control gains $\mathbf{K}_{sf}$, for the state feedback internal loop, and $\mathbf{T}_d$, for the resonant control external loop, is detailed below.

A. Step 1: internal loop design

In order to design the internal loop, consider the control signal in Fig. 3, given by

$$\mathbf{u}_{sf}(k) = -\mathbf{K}_{sf}\mathbf{x}_d(k) + u_r(k) \tag{10}$$

where the state feedback control gains are given by

$$\mathbf{K}_{sf} = [K_{ic}\ \ K_{vc}\ \ K_{ig}\ \ K_{\phi}] \tag{11}$$

From (5) and (10), one can write

$$\begin{aligned} &\mathbf{x}_d(k+1) = \mathbf{G}_{cl}\mathbf{x}_d(k) + \mathbf{H}_{ud}\mathbf{u}_r(k) + \mathbf{H}_{gd}v_g(k), \\ &\mathbf{G}_{cl} = \mathbf{G}_d - \mathbf{H}_{ud}\mathbf{K}_{sf} \end{aligned} \tag{12}$$

Thus, if the pair ($\mathbf{G}_d$,$\mathbf{H}_{ud}$) is controllable, the eigenvalues of the state matrix of the inner loop, given by $\mathbf{G}_{cl}$, in (12), can be assigned by the suitable computation of the gains in (11) using, for instance, the Ackermann's formula [14]

$$\mathbf{K}_{sf} = [0\ 0\ 0\ 1]\mathscr{C}^{-1}\Delta(\mathbf{G_d}) \tag{13}$$

where $\mathscr{C}$ is the controllability matrix and $\Delta(\mathbf{G_d})$ is the closed-loop characteristic polynomial in terms of the matrix $\mathbf{G}_d$.

If the designer chooses the closed-loop eigenvalues, that is, the eigenvalues of $\mathbf{G}_{cl}$, for instance, with pure real positive values inside the unit circle, the poles of the plant with delay will be damped, and the resonance peak from the LCL filter profile can be attenuated by the controller in the internal loop.

B. Step 2: external loop design

Now, assume that the inner loop was already designed, that is, the gain vector $\mathbf{K}_{sf}$ was computed to damp the resonance of the plant discretized with delay. Taking into account the outer loop resonant controller (7), one can write the augmented model

$$\begin{bmatrix} \mathbf{x}_d(k+1) \\ \boldsymbol{\rho}(k+1) \end{bmatrix} = \begin{bmatrix} \mathbf{G}_{cl} & \mathbf{H}_{ud}\mathbf{T}_d \\ -\mathbf{S}_d\mathbf{C}_d & \mathbf{R}_d \end{bmatrix} \begin{bmatrix} \mathbf{x}_d(k) \\ \boldsymbol{\rho}(k) \end{bmatrix} + \begin{bmatrix} \mathbf{H}_{gd} \\ \mathbf{0} \end{bmatrix} v_g(k) + \begin{bmatrix} \mathbf{0} \\ \mathbf{S}_d \end{bmatrix} r(k) \tag{14}$$

$$y(k) = \begin{bmatrix} \mathbf{C}_d(k) & \mathbf{0} \end{bmatrix} \begin{bmatrix} \mathbf{x}_d(k) \\ \boldsymbol{\rho}(k) \end{bmatrix}$$

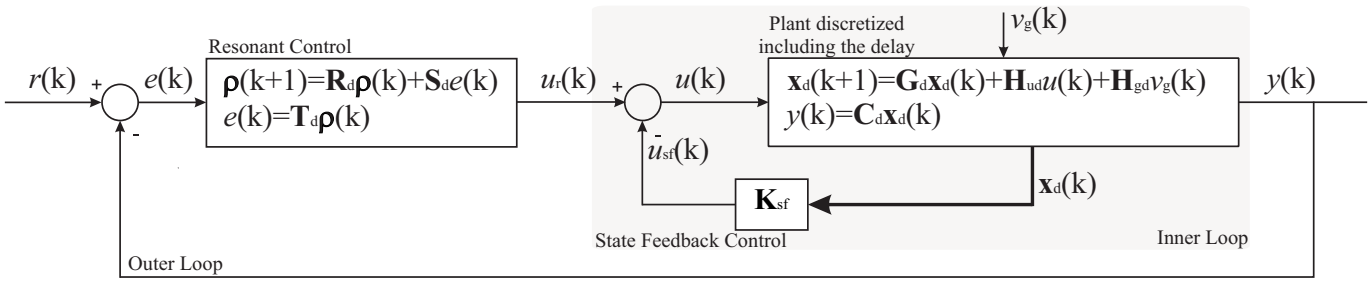

Figure 3. Control system for grid current regulation. Internal loop: state feedback control with gain $\mathbf{K_{sf}}$. External loop: resonant control, with gain $\mathbf{T_d}$.

Notice that the model (14) depends on the gain vector $\mathbf{T}_d$, of the resonant controller, to be computed to attain some control objective.

Due to the importance of the time response of this control system in the tracking of sinusoidal references, here the control vector $\mathbf{T}_d$ will be obtained from the minimization of the integral time squared error (ITSE) for the reference profile given in Fig. 4.

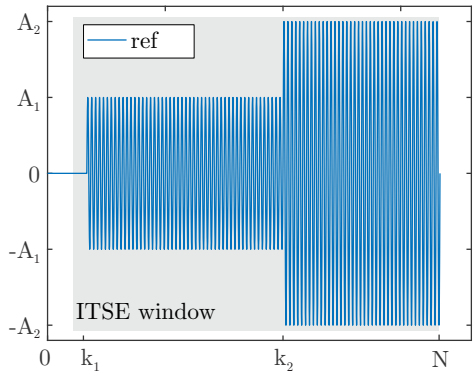

Figure 4. Reference profile for the grid current to test the closed-loop system tracking capacity.

Notice that the reference in Fig. 4 begins with zero value, changes the amplitude to an intermediate peak value, and then changes the amplitude to a value related with the nominal power of the GCC, for instance. This reference can be written as

$$i_{g_{ref}}(k) = \begin{cases} 0, & 0 < k < k_1 \\ A_1 \sin(2\pi \mathrm{f_{grid}} k), & k_1 < k < k_2 \\ A_2 \sin(2\pi \mathrm{f_{grid}} k), & k \geq k_2 \end{cases} \quad (15)$$

where k_1, k_2, f_{grid}, A_1 and A_2 are chosen by the control designer.

The ITSE ctriterion can be computed as

$$\mathrm{ITSE} = \sum_{k=0}^{N} k\,(r(k) - i_g(k))^2 \quad (16)$$

The resonant controller gain vector, of the outer loop, can be computed based on the minimization of the ITSE criterion. In this case, the gain vector $\mathbf{T}_d$ can be obtained by a searching procedure in a previously given set, $\mathscr{T}$, in the optimization problem

$$\mathbf{T}_d = \arg\min_{\mathscr{T}} \mathrm{ITSE} \quad (17)$$

In the next section, a case study is given, to illustrate the computation of $\mathbf{K}_{sf}$ and $\mathbf{T}_d$, for a GCC with parameters in the literature.

IV. Case Study

For a case study, consider the parameters of GCC with LCL filter borrowed from [16]–[20], given in Table I.

Table I
GCC WITH LCL FILTER PARAMETERS.

LCL filter converter side inductance	L_c	1 mH
LCL filter capacitance	C_f	62 uF
LCL filter grid side inductance	L_{g1}	0.3 mH
Grid Inductance minimum value	$L_{g2_{min}}$	0 mH
Grid Inductance maximum value	$L_{g2_{max}}$	1 mH
Grid voltage	v_g	127 V, 60 Hz
Sampling frequency	f_s	20040 Hz

For sake of the design of the control gains, it is considered as the nominal plant the one related with L_{g2min}. Nevertheless, any other value of L_{g2} between L_{g2min} and L_{g2max} could be used in the proposed design procedure.

Applying Step 1 of the proposed procedure, with the choice of closed-loop eigenvalues at $[0.7, 0.7, 0.7, 0.1]$ to minimize the resonance peak, using the function *acker*, from MATLAB©, one has the state feedback control gains

$$\mathbf{K_{sf}} = [13.18 \quad -0.86 \quad -9.51 \quad 0.62] \quad (18)$$

The frequency response of the open-loop plant discretized with the delay, in (5), for both situations of L_{g2} are given in Fig. 5. It can be noticed the peak of the resonance of the LCL filter, and its change with the change in the value of the grid inductance. In the same figure, one has the responses of the closed-loop system with the state feedback control action (i.e., only the effect of the internal control loop). It becomes clear the damp of the resonance of the filter, in both grid inductance conditions, thanks to the state feedback gains.

Now, taking into account the internal loop gains $\mathbf{K}_{sf}$ in (18), and applying Step 2 of the proposed procedure, for a

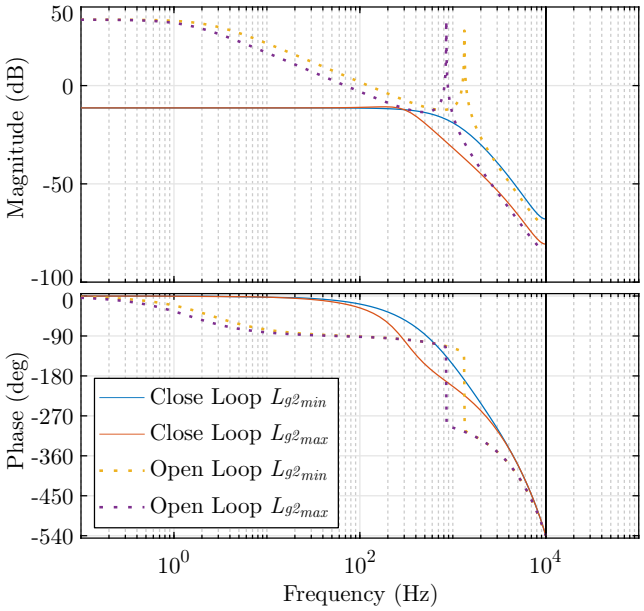

Figure 5. Bode diagrams for the open-loop plant and for the closed-loop plant with active damping.

search space of K_{r1} and K_{r2} between -20 and 20, one has that $\mathbf{T_d} = [K_{r1}\ K_{r2}]$ has entries given by

$$\mathbf{T_d} = [15.04\ \ -15.00] \tag{19}$$

This control gain vector minimizes the ITSE criterion defined in the previous section, and was found by means of an exhaustive search.

The closed-loop responses with state feedback and resonant controller, simulated with parameters in Table I, are shown in Fig.6, for both grid inductance conditions. It is possible to notice the good tracking of the reference, with fast transient responses against reference variations and suitable steady state. These properties were obtained due to the optimization of the ITSE criterion.

Finally, to confirm the robust stability of the closed-loop system with the internal and external control loops, a sweep in the eigenvalues is shown in Fig. 7. It is possible to see that all the closed-loop eigenvalues of system (14) remain inside the unit circle, for values of grid inductance L_{g2} inside the grid uncertainty interval in Table I, corroborating the stable behavior.

V. Conclusion

This paper provided a two step procedure for the current control design applied to grid-connected converters with LCL filters. The first step of the proposed procedure is to compute state feedback control gains using a pole location strategy, aiming to suitably damp the resonance peak of the LCL filter, taking into account the one sample delay. Then the gains of a resonant controller in the outer loop are computed based on the minimization of the grid current tracking error, given a sinusoidal reference pattern. Typical parameters from the literature were used to provide a case study, which illustrated

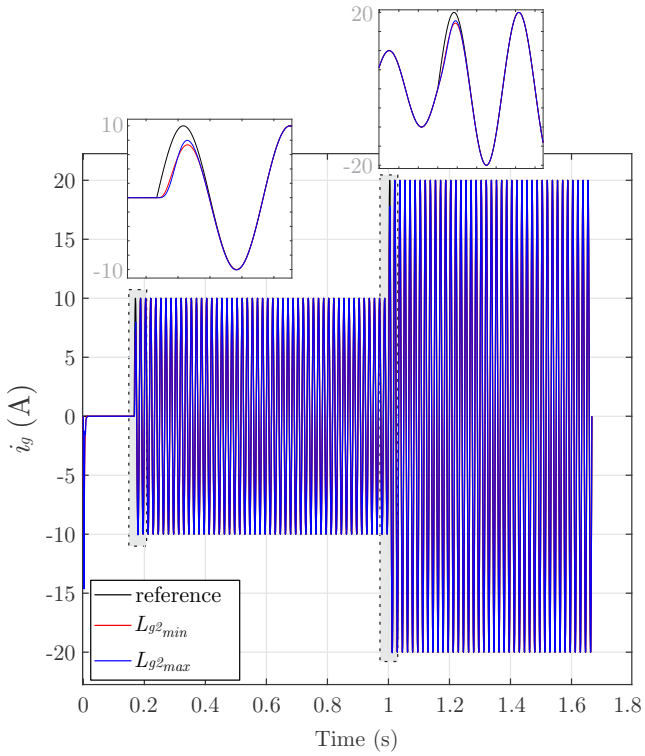

Figure 6. Time responses of the closed-loop system with the two control loops, for operation with grid inductances L_{g2min} and L_{g2max}.

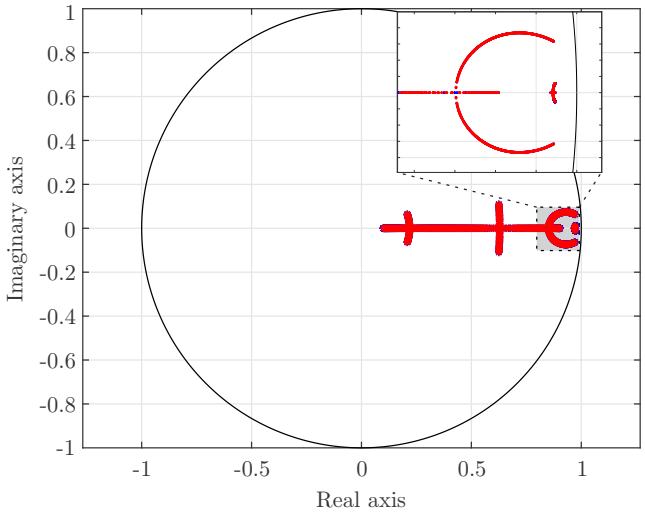

Figure 7. Eigenvalues of the closed-loop system with the two control loops, for a sweep in the values of L_{g2} from L_{g2min} to L_{g2max}.

that the proposed procedure allows to get control gains for the two control loops, ensuring closed-loop systems with suitable grid currents for this important class of power converters.

VI. Acknowledgments

This study was financed in part by the Coordenação de Aperfeiçoamento de Pessoal de Nível Superior - Brasil (CAPES/PROEX) - Finance Code 001. The authors also thank to INCT-GD, CNPq (465640/2014-1, 309536/2018-9), CAPES

(23038.000776/2017-54), and FAPERGS (17/2551-0000517-1).

REFERENCES

[1] F. Blaabjerg, R. Teodorescu, M. Liserre, and A. Timbus, "Overview of Control and Grid Synchronization for Distributed Power Generation Systems," IEEE Transactions on Industrial Electronics, vol. 53, no. 5, pp. 1398 –1409, oct. 2006.

[2] I. J. Gabe, V. F. Montagner, and H. Pinheiro, "Design and Implementation of a Robust Current Controller for VSI Connected to the Grid Through an LCL Filter," IEEE Transactions on Power Electronics, vol. 24, no. 6, pp. 1444–1452, June 2009.

[3] J. Dannehl, F. Fuchs, S. Hansen, and P. Thøgersen, "Investigation of Active Damping Approaches for PI-Based Current Control of Grid-Connected Pulse Width Modulation Converters With LCL Filters," Industry Applications, IEEE Transactions on, vol. 46, no. 4, pp. 1509 –1517, july-aug. 2010.

[4] R. Teodorescu, M. Liserre, and P. Rodríguez, Grid Converters for Photovoltaic and Wind Power Systems, ser. Wiley - IEEE. John Wiley & Sons, 2011.

[5] V. Miskovic, V. Blasko, T. Jahns, A. Smith, and C. Romenesko, "Observer Based Active Damping of LCL Resonance in Grid Connected Voltage Source Converters," in Energy Conversion Congress and Exposition (ECCE), 2013 IEEE, Sept 2013, pp. 4850–4856.

[6] J. He, Y. W. Li, D. Bosnjak, and B. Harris, "Investigation and Active Damping of Multiple Resonances in a Parallel-Inverter-Based Microgrid," Power Electronics, IEEE Transactions on, vol. 28, no. 1, pp. 234 –246, jan. 2013.

[7] J. Xu, S. Xie, and T. Tang, "Active Damping-Based Control for Grid-Connected LCL -Filtered Inverter With Injected Grid Current Feedback Only," Industrial Electronics, IEEE Transactions on, vol. 61, no. 9, pp. 4746–4758, Sept 2014.

[8] M. Hanif, V. Khadkikar, W. Xiao, and J. Kirtley, "Two Degrees of Freedom Active Damping Technique for LCL Filter-Based Grid Connected PV Systems," Industrial Electronics, IEEE Transactions on, vol. 61, no. 6, pp. 2795–2803, June 2014.

[9] M. Su, B. Cheng, Y. Sun, Z. Tang, B. Guo, Y. Yang, F. Blaabjerg, and H. Wang, "Single-Sensor Control of LCL-Filtered Grid-Connected Inverters," IEEE Access, vol. 7, pp. 38 481–38 494, 2019.

[10] R. A. Fantino, C. A. Busada, and J. A. Solsona, "Observer-Based Grid-Voltage Sensorless Synchronization and Control of a VSI-LCL Tied to an Unbalanced Grid," IEEE Transactions on Industrial Electronics, vol. 66, no. 7, pp. 4972–4981, July 2019.

[18] G. G. Koch, L. A. Macari, R. Oliveira, and V. F. Montagner, "Robust $\mathscr{H}_\infty$ State Feedback Controllers based on LMIs applied to Grid-Connected Converters," IEEE Transactions on Industrial Electronics, vol. 66, no. 8, pp. 6021–6031, 2019.

[11] C. S. Lim, S. S. Lee, I. U. Nutkani, X. Kong, and H. H. Goh, "Near-Optimal MPC Algorithm for Actively Damped Grid-Connected PWM-VSCs With LCL Filters," IEEE Transactions on Industrial Electronics, vol. 67, no. 6, pp. 4578–4589, 2020.

[12] X. Chen, W. Wu, N. Gao, H. S. Chung, M. Liserre, and F. Blaabjerg, "Finite Control Set Model Predictive Control for LCL-Filtered Grid-Tied Inverter With Minimum Sensors," IEEE Transactions on Industrial Electronics, vol. 67, no. 12, pp. 9980–9990, 2020.

[13] J. Zhao, W. Wu, Z. Shuai, A. Luo, H. S. Chung, and F. Blaabjerg, "Robust Control Parameters Design of PBC Controller for LCL-Filtered Grid-Tied Inverter," IEEE Transactions on Power Electronics, vol. 35, no. 8, pp. 8102–8115, Aug 2020.

[14] R. C. Dorf and R. H. Bishop, Modern control systems, 11th ed. Upper Saddle River, USA: Prentice Hall, 2008.

[15] K. Zhou, J. C. Doyle, and K. Glover, Robust and Optimal Control. Upper Saddle River, NJ, USA: Prentice Hall, 1996.

[16] V. F. Montagner, L. A. Maccari, G. G. Koch, J. R. Massing, H. Pinheiro, A. A. Ferreira, and R. C. L. F. Oliveira, "Partial State Feedback Controllers Applied to Grid-Connected Converters," in 2015 IEEE 13th Brazilian Power Electronics Conference and 1st Southern Power Electronics Conference (COBEP/SPEC), Nov 2015, pp. 1–4.

[17] G. G. Koch, L. A. Maccari, J. R. Massing, H. Pinheiro, R. C. L. F. Oliveira, and V. F. Montagner, "Robust Control Based on State Observer Applied to Grid-Connected Converters," in 2016 12th IEEE International Conference on Industry Applications (INDUSCON), Nov 2016, pp. 1–6.

[19] C. R. Osório, G. G. Koch, R. C. Oliveira, and V. F. Montagner, "A Practical Design Procedure for Robust $\mathscr{H}_2$ Controllers Applied to Grid-Connected Inverters," Control Engineering Practice, vol. 92, p. 104157, 2019.

[20] C. R. D. Osório, G. G. Koch, H. Pinheiro, R. C. L. F. Oliveira, and V. F. Montagner, "Robust Current Control of Grid-Tied Inverters Affected by LCL Filter Soft-Saturation," IEEE Transactions on Industrial Electronics, vol. 67, no. 8, pp. 6550–6561, August 2019.

[21] R. Peña-Alzola, M. Liserre, F. Blaabjerg, R. Sebastián, J. Dannehl, and F. W. Fuchs, "Analysis of the Passive Damping Losses in LCL-Filter-Based Grid Converters," IEEE Transactions on Power Electronics, vol. 28, no. 6, pp. 2642 –2646, june 2013.

[22] R. Pena-Alzola, M. Liserre, F. Blaabjerg, R. Sebastian, J. Dannehl, and F. Fuchs, "Systematic Design of the Lead-Lag Network Method for Active Damping in LCL-Filter Based Three Phase Converters," Industrial Informatics, IEEE Transactions on, vol. 10, no. 1, pp. 43–52, Feb 2014.

[23] K. Aström and B. Wittenmark, Computer-Controlled Systems: Theory and Design. Prentice Hall, 1997.